

CFD ANALYSIS OF INLET AND OUTLET REGIONS OF COOLANT CHANNELS IN AN ADVANCED HYDROCARBON ENGINE NOZZLE

TFAWS04 PAPER 109-A0019

15th ANNUAL THERMAL & FLUIDS ANALYSIS WORKSHOP
AUGUST 30TH – SEPTEMBER 3RD
NASA-JPL PASADENA, CA, USA

Dr. Kevin R. Anderson,
Associate Professor
Department of Mechanical Engineering
California State Polytechnic University at Pomona
3801 West Temple Ave
Pomona, CA 91768
USA
909-869-2687
FAX 909-869-4341
kranderson1@csupomona.edu

Thermal / Fluids Engineer,
Swales Aerospace

Faculty Part-Time Thermal & Fluids Systems Engineering Group,
NASA JPL

ABSTRACT

In this paper, FLUENT CFD software is used to simulate the flow of supercritical nitrogen coolant around an experimental rocket engine nozzle configuration. The ultimate goal of this research is to build a one million pound thrust rocket engine. The CFD analysis presented herein focuses on the inlet and outlet regions to the coolant passages in the wall of the combustion chamber where the flow diverges or converges while making a 90 degree turn. In these regions of the flow, the fluid is stagnant, causing a reduction in the convective film coefficient. The heat flux from the combustion chamber is so large, that even a small region of low convective heat transfer could result in a significant local increase in the combustion chamber wall temperature, potentially leading to thermally induced structural failure. GAMBIT 2.0 /FLUENT 6.0 3-D Finite Volume CFD code using the $k-\varepsilon$ model and the NIST-12 database to model the supercritical nitrogen as a user defined fluid is employed for this analysis. Results presented include the film coefficient as a function of coolant flow rate and flow regime velocity fields. The main findings of this investigation are as follows. For a 71% increase in coolant flow rate, one achieves a 65% increase in heat transfer capability. The ratio of convective film coefficients at the inlet and outlet regions is approximately, $\frac{h_{inlet}}{h_{outlet}} \cong 3$.

NOMENCLATURE

ACRONYMS

AHEP	Advanced Hydrocarbon Engine Program
AMG	Algebraic Multigrid Method
CFD	Computational Fluid Dynamics
NIST	National Inst. of Standards and Technology
SIMPLE	Semi-Implicit-Method for Pressure-Linked-Equations
TKE	Turbulent Kinetic Energy

VARIABLES

A	Channel flow area
Br	Brinkman Number
c	Speed of sound
c_p	Specific heat capacity of fluid at const. pressure
$C_{1\varepsilon}, C_{2\varepsilon}, C_\mu$	Turbulence model constants
D_h	Channel hydraulic diameter
E	Total energy of the fluid
h	Convective film coefficient, fluid specific enthalpy

h_{inlet}	Convective film coefficient at inlet region of channel
h_{outlet}	Convective film coefficient at outlet region of channel
\bar{h}	Area weighted average convective film coefficient
h_j	Specific sensible enthalpy
\tilde{I}	Identity tensor
k	Turbulent Kinetic Energy, fluid heat conductivity
k_{eff}	Effective thermal conductivity
\dot{m}	LN2 coolant mass flow rate
Ma	Mach Number
p	Fluid pressure
P	Channel flow perimeter
Re	Reynolds Number based on hydraulic diameter
T	Fluid temperature
u	Local flow velocity in x – direction (streamwise)
u_i	Tensor shorthand notation for mean velocity field
u'_i	Tensor shorthand notation for turbulent velocity field
\vec{U}	Fluid velocity vector
Y_j	Mass fraction

GREEK

ε	Rate of dissipation of TKE
r	Fluid density
μ	Fluid absolute viscosity
μ_t	Turbulent viscosity
$\sigma_t, \sigma_\varepsilon$	Turbulent model constant
$\tilde{\tau}$	Viscous stress tensor
$\tilde{\tau}_{eff}$	Effective viscous stress tensor

INTRODUCTION

The motivation for this problem stemmed from the Advanced Hydrocarbon Engine Program (AHEP) sponsored by the Air Force. Swales Aerospace was contracted to support design validation of the combustion chamber for the AHEP program. The objectives of the present Computational Fluid Dynamics (CFD) analysis were to characterize the flow field within the inlet and outlet regions of the coolant channel and evaluated the variance film heat transfer coefficient as a function of coolant

supply rate. Supercritical nitrogen is used as the working coolant which is plumbed around a converging-diverging combustion nozzle which comprises the structure of a prototype hydrocarbon engine. Figure 1 shows a prototype engine in a test stand.

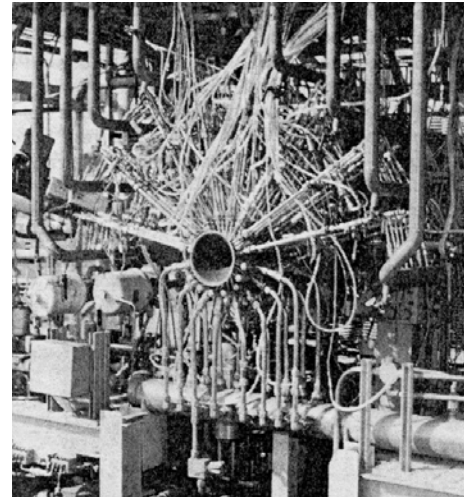


Figure 1. AHEP Prototype Engine in Test Stand

The combustion chamber is a cylindrical chamber narrowing down to a throat region as shown in Figure 2.

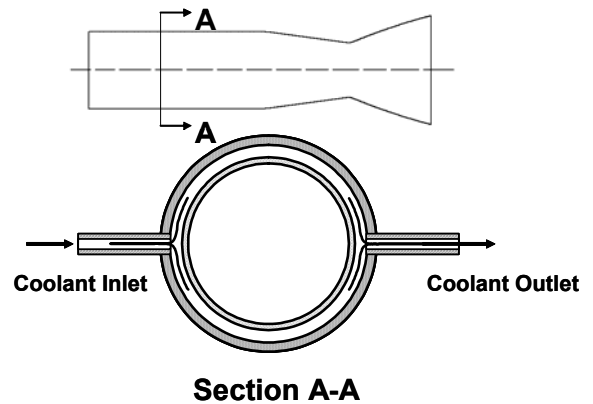


Figure 2. Combustor geometry

The chamber has a copper combustor liner with an electroformed nickel closeout and an injector mounting flange at one end. The chamber is cooled by a coolant (supercritical N₂) circulating in a series of annular rings surrounding the copper liner. The coolant enters the inlet at one end at a pressure of 6000 psi, and splits into two paths. The two paths merge at the outlet and the coolant exits at 4000 to 4500 psi.

For the configuration of the coolant channels shown in Figure 2, the mixing of the two flow branches at the outlet will lower the heat transfer film coefficient. It was required to the

variation of the heat transfer coefficient as a function of the flow rate in order to ensure satisfactory coolant performance. If the coolant heat removal rate is too small, exceedingly large thermally induced stresses in the combustor wall could lead to catastrophic failure of the engine. This, the CFD analysis was used to predict the local convective film heat transfer coefficient along the length of the channel, for various flow rates. Details of the coolant channel geometry are shown in Figure 3.

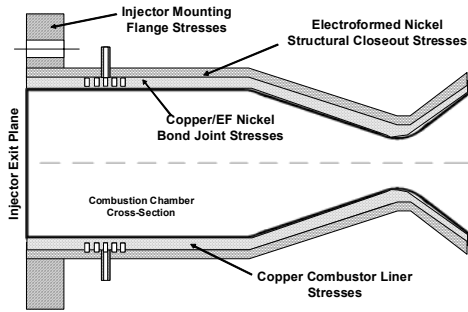


Figure 3. Combustor wall cross-sectional view

A coolant channel has the typical dimensions shown below in Figure 4.

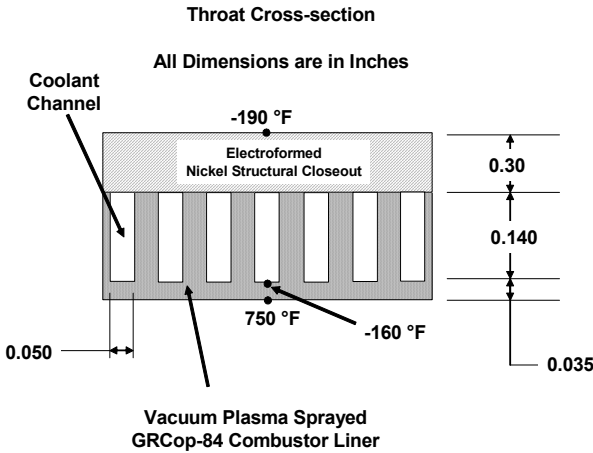


Figure 4. Combustor throat cross-sectional view

Figure 4 also illustrates the typical values of temperature witnessed by the various material components of the composite combustor wall.

CFD MODEL DEVELOPMENT

The coolant channel at the location of the combustor having the minimum throat diameter was selected for detailed CFD analysis. The methodology being that if the smallest diameter coolant channel could remove enough heat from the chamber, than neighboring channels possessing larger heat transfer surface area would perform sufficiently. Thus, the analysis

herein is a bounding analysis, dealing only with the coolant channel of least inner and outer diameter.

Prior to the onslaught of exhaustive computer based CFD calculations, bounding hand calculations were used to justify the CFD model assumptions. First, based upon inlet typical flow rates, LN2 properties and using the channel dimensions of Figure 4, the inlet and outlet Reynolds Numbers of the channel were computed. The LN2 properties were taken from the NIST 12 thermo-physical properties database program [1]. Reynolds numbers were computed based upon an equivalent diameter for the channel as follows

$$Re = \frac{4\dot{m}}{\pi\mu D_h} \quad (1)$$

where the hydraulic diameter is defined as

$$D_h = \frac{4A}{P} \quad (2)$$

where A is the cross-sectional area of the channel, based upon it's height and width, and P is the perimeter of the channel. The parameters \dot{m} and μ appearing in Eqn (1) are the mass flow rate of LN2, and the absolute viscosity of LN2, respectively. For the analysis herein, the values of the inlet and outlet Reynolds number were computed as summarized in Table 1.

Table 1. Reynolds Numbers of channel inlet and outlet

Flow Rate (lb/s)	Re inlet $\times 10^5$	Re outlet $\times 10^5$
0.7	0.815	38.6
1.0	1.165	55.1
1.2	1.398	66.1

The hand-calculations of Table 1 are based upon in inlet supply of LN2 at 6000 psia, 140 R, and an outlet LN2 at 4870 psi, 285 R. These inlet and outlet state points were used for the remainder of the bounding analysis discussed herein.

Inspection of the Reynolds numbers listed in Table 1, lead us to conclude that the internal flow at hand should be modeled as a turbulent flow. This assumption was verified by using the critical Reynolds number, $Re_{trans} \sim 2300$ for flow in a circular channel. Note, that when dealing with rectangular channels, such as the one at hand, the above value for the transitional Reynolds number holds provided that the aspect ratio of the channel is less than about 3 or 4 [2]. For the geometry studied herein, the aspect ratio $\frac{h}{w} < 3$, thus the

Reynolds numbers of Table 1 indicate turbulent flow with respect to a transition Reynolds number of 2300.

The next bounding calculation determined if the flows at hand could best be modeled as either incompressible or compressible flows. Using the definition of the Mach Number

$$Ma = \frac{u}{c} = \frac{\dot{m}}{\rho A c} \quad (3)$$

and corresponding values of the working fluid at the inlet and outlet ports, the Mach numbers found in Table 2 were computed.

Table 2. Mach Numbers of channel inlet and outlet

Flow Rate (lb/s)	<i>Ma</i> inlet	<i>Ma</i> outlet
0.7	0.073	0.171
1.0	0.105	0.244
1.2	0.126	0.293

Clearly, the flow is sub-sonic in all instances, since $Ma < 1$. Thus, the flow was modeled as incompressible.

The grid of the channel was constructed using GAMBIT 2.0 software. Figure 5 below illustrates the outline of the structured mesh of the coolant channel used in the CFD computations.

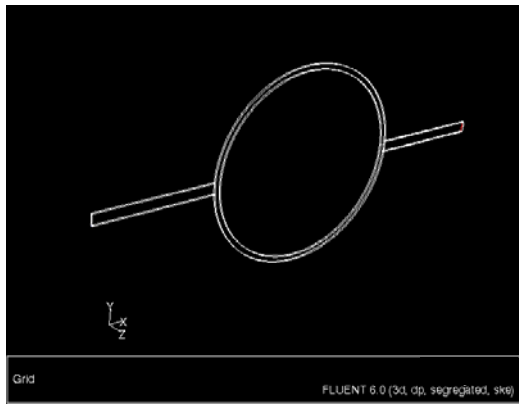


Figure 5. Outline of CFD mesh

Figures 6 and 7 depict detailed views of the structured mesh of the inlet and outlet regions of the coolant channel, respectively.

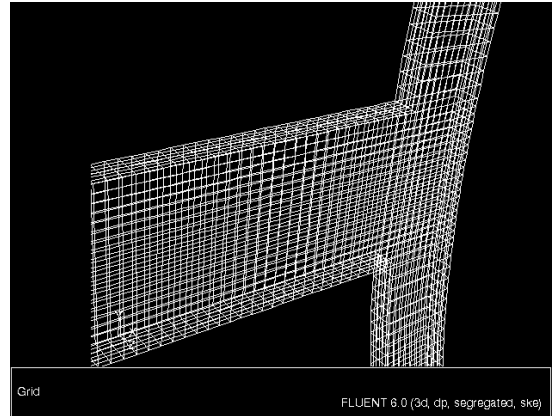


Figure 6 CFD mesh near inlet region

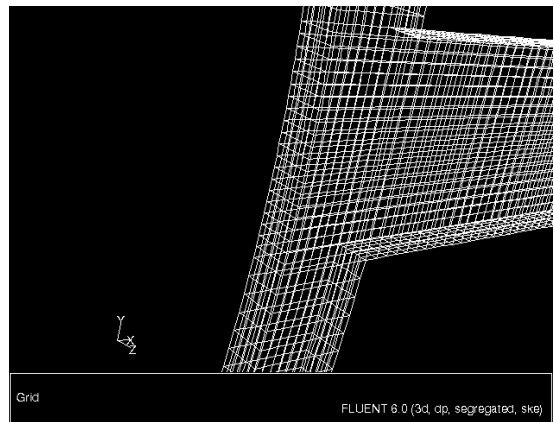


Figure 7 CFD mesh near inlet region

EQUATIONS OF MOTION:

FLUENT 6.0 unsteady segregated solver using with second-order upwind spatial discretization and SIMPLE pressure-velocity coupling was used for the computations [3]. The flow was modeled as incompressible, turbulent, viscous flow with internal heat transfer. The standard $k-\epsilon$ model was used to model the turbulence. The equations of motion solved are as follows (the reader is referred to the nomenclature section of this paper for the definition of the various quantities which follow):

Conservation of Mass:

$$\frac{\partial \rho}{\partial t} + \nabla \cdot (\rho \vec{v}) = 0 \quad (4)$$

Conservation of Momentum:

$$\frac{\partial(\rho\bar{v})}{\partial t} + \nabla \cdot (\rho\bar{v}\bar{v}) = -\nabla p + \nabla \cdot \tilde{\tau} \quad (5)$$

$$\tilde{\tau} = \mu \left[(\nabla\bar{v} + \nabla\bar{v}^T) - \frac{2}{3} \nabla \cdot \bar{v} \tilde{I} \right] \quad (6)$$

Conservation of Energy:

$$\frac{\partial(\rho E)}{\partial t} + \nabla \cdot [\bar{v}(\rho E + p)] = \nabla \cdot [k_{eff} \nabla T - \tilde{\tau}_{eff} \cdot \bar{v}] \quad (7)$$

$$E = h - \frac{p}{\rho} + \frac{v^2}{2} \quad (8)$$

$$h = \sum_j Y_j h_j + \frac{p}{\rho} \text{ for incompressible flows} \quad (9)$$

$$h_j = \int_{T_{ref}}^T c_{p,j} dT \quad T_{ref} = 298.15 \text{ K} \quad (10)$$

By default, for incompressible flows, when using the segregated solver in FLUENT, the pressure work and kinetic energy terms of the energy equation are not included, since they are negligible. The viscous dissipation terms which describe thermal energy created by the viscous shear in the flow must be included in the analysis depending upon the value of the Brinkman number, Br . The criteria is if,

$$Br = \frac{\mu u_{stream}^2}{k \Delta T} > 1 \quad (11)$$

then viscous dissipation terms must be modeled in the energy equation. For the internal convective heat transfer problem considered herein, $Br \sim 1.14, 2.3, 3.4$ for the given flow rates, thus, viscous heating was activated in the FLUENT CFD model.

The standard $k-\varepsilon$ turbulence model is given as follows:

$$\frac{\partial(\rho k)}{\partial t} + \frac{\partial(\rho k u_i)}{\partial x_i} = \frac{\partial}{\partial x_j} \left[\left(\mu + \frac{\mu_t}{\sigma_k} \right) \frac{\partial k}{\partial x_j} \right] - \rho \overline{u_i' u_j'} \frac{\partial u_j}{\partial x_i} - \rho \varepsilon \quad (12)$$

$$\begin{aligned} \frac{\partial(\rho \varepsilon)}{\partial t} + \frac{\partial(\rho \varepsilon u_i)}{\partial x_i} = & \frac{\partial}{\partial x_j} \left[\left(\mu + \frac{\mu_t}{\sigma_\varepsilon} \right) \frac{\partial \varepsilon}{\partial x_j} \right] \\ & - C_{1\varepsilon} \frac{\varepsilon}{k} \left(\rho \overline{u_i' u_j'} \frac{\partial u_j}{\partial x_i} \right) - C_{2\varepsilon} \frac{\varepsilon^2}{k} \end{aligned} \quad (13)$$

Where the turbulent eddy viscosity is given by:

$$\mu_t = \rho C_\mu \frac{k^2}{\varepsilon} \quad (14)$$

and the following default values of the $k-\varepsilon$ turbulence model constants are taken:

$$C_{1\varepsilon} = 1.44, C_{2\varepsilon} = 1.92, C_\mu = 0.09$$

$$\sigma_k = 1.0, \sigma_\varepsilon = 1.3$$

The FLUENT 6.0 segregated solver, which means that the governing equations are solved sequentially, i.e. segregated from one another. SIMPLE is the default pressure-velocity coupling employed in FLUENT. Because the governing equations are non-linear (and coupled), many iterations of the solution loop must be performed before a converged solution is obtained. The process is depicted in Figure 8 below:

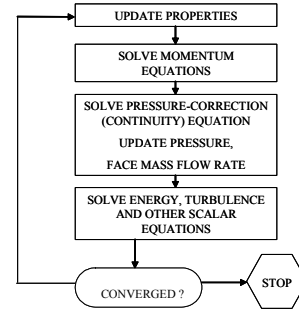


Figure 8. FLUENT segregated solver flow-chart

FLUENT 6.0 utilizes a Finite Volume discretization of the governing equations. Implicit linearization of the discretized equations results in a system of linear equations for each cell in the domain. Point implicit Gauss-Seidel linear equation solver used in conjunction with an Algebraic Multigrid Method (AMG) to solve the resultant scalar system of equations. Mesh independence studies performed on the channel flow grid showed approximately that 70,000 Finite Volumes were required for grid independent converged results.

In order to model LN2, a user defined fluid had to be set up within FLUENT, since LN2 was not provided as a default fluid at the time of this analysis. The NIST 12 database [1] was used to construct curve fits of the various flow quantities needed:

$\rho, h, s, c_p, c_v, k, \mu$ These curve fits were input into FLUENT using the coefficients found from EXCEL polynomial fits of the property data over the expected range of temperature and pressure for the simulations at hand. A typical set of curve fits for LN2 fluid density is shown in Figure 9.

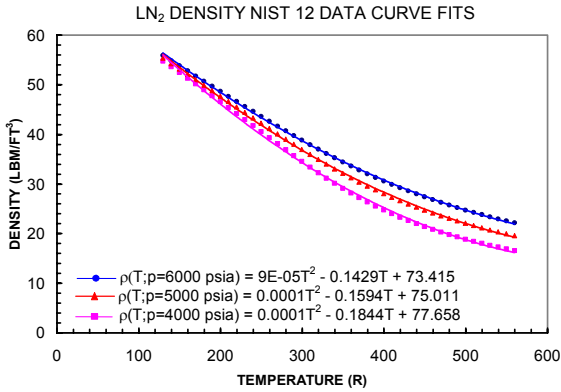
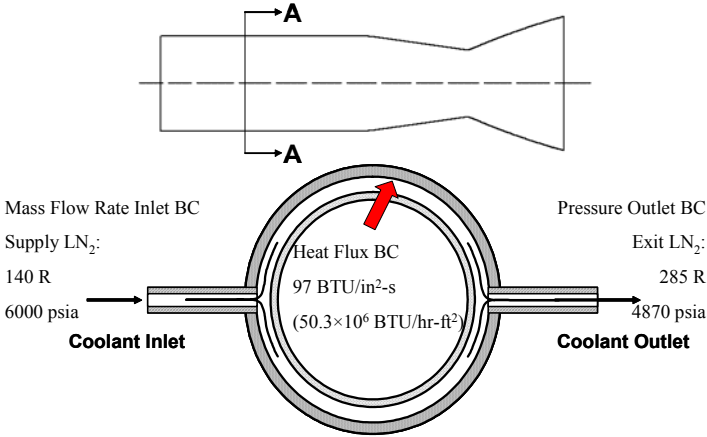


Figure 9. Curve fit of NIST 12 LN2 fluid density used as inputs to FLUENT user defined fluid

BOUNDARY CONDITIONS

The boundary conditions are depicted in Figure 10.



Section A-A

Figure 10. Boundary conditions used for coolant channel CFD simulations.

The interior walls of the combustor were modeled as no-slip wall boundary conditions, whose temperatures were computed by FLUENT. The heat flux boundary condition was applied at the inner diameter of the combustion chamber and applied as a constant value over the duration of the simulations. Neglecting the conduction thru the inner wall of the combustion chamber allows us to avoid solving the conjugate heat transfer problem. This assumption is warranted, given the relatively large value of heat flux prescribed along the very thin inner wall of the combustion chamber, 50×10^6 BTU/hr-ft². The inlet boundary condition is a mass flow rate boundary condition. To avoid edge effects due to numerical modeling, the inlet and outlet are assumed to be comprised of several hydraulic diameter lengths of duct length, both held at isothermal wall conditions. This in effect “conditions” the fluid before it meets the fork between top and bottom branches of the combustor channel. The exit boundary condition is a far-field pressure boundary condition. Using several hydraulic diameters downstream of the exit as

also aids in the numerical convergence of the problem when imposing a far-field pressure boundary condition.

RESULTS

Velocity vectors near inlet, velocity vectors near outlet, overall contour map of convective film coefficient, and zoomed in regional contours of convective film coefficient near inlet and outlet are shown in Figures 12-24, for the three nominal flow rates of 0.7, 1.0 and 1.2 lb/s, respectively. For even the most extreme flow rate, 1.2 lb/s the local velocity field maximum achieves a value of 416 ft/s at the inlet (see Figure 21). This confirms that the flow is sub-sonic since the local speed of sound of LN2 at 6000 psia and 140 R is approximately 3580 ft/s.

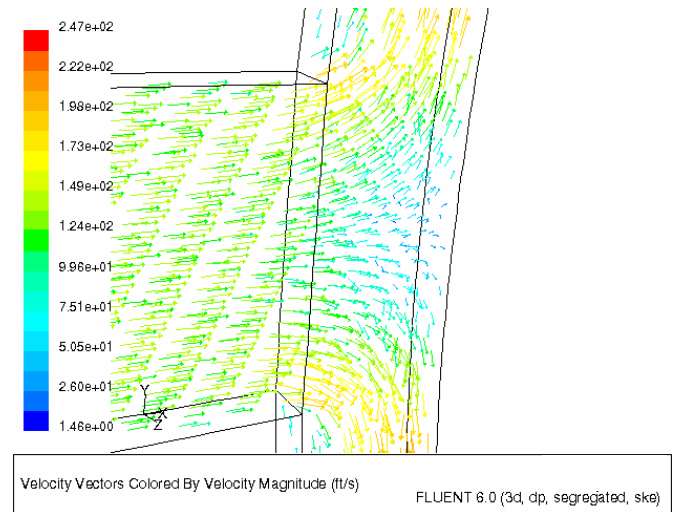


Figure 11. Flow rate = 0.7 lb/s velocity vectors near inlet.

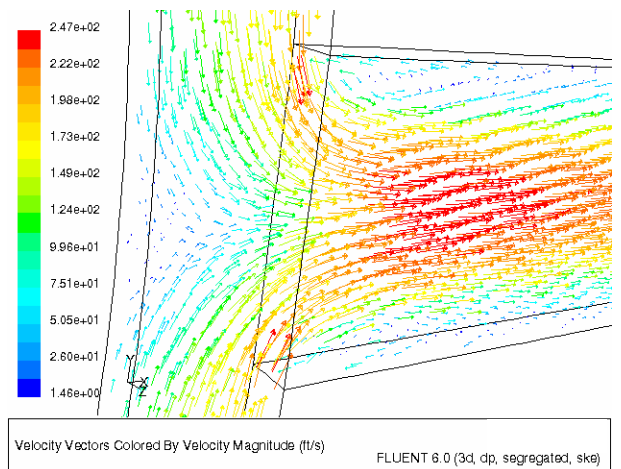


Figure 12. Flow rate = 0.7 lb/s velocity vectors near outlet.

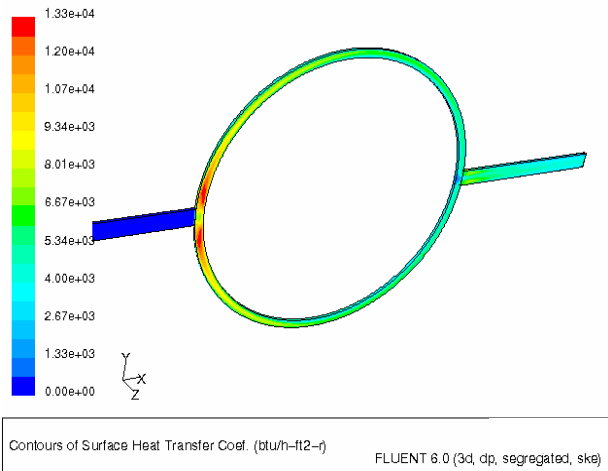


Figure 13. Flow rate = 0.7 lb/s contours of h (BTU/hr-ft²-R).

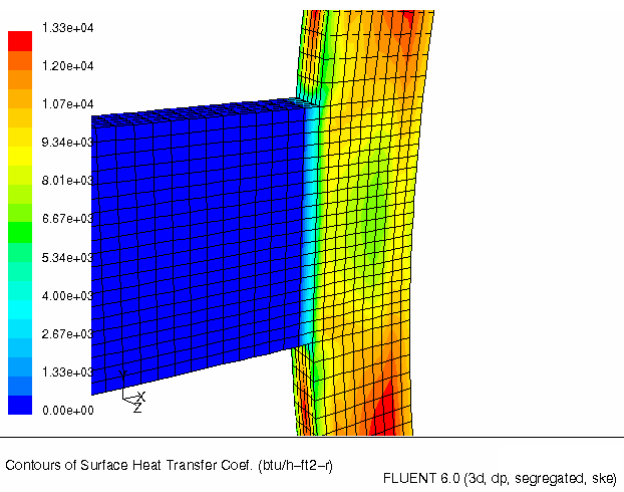


Figure 14. Flow rate = 0.7 lb/s contours of h (BTU/hr-ft²-R) near inlet.

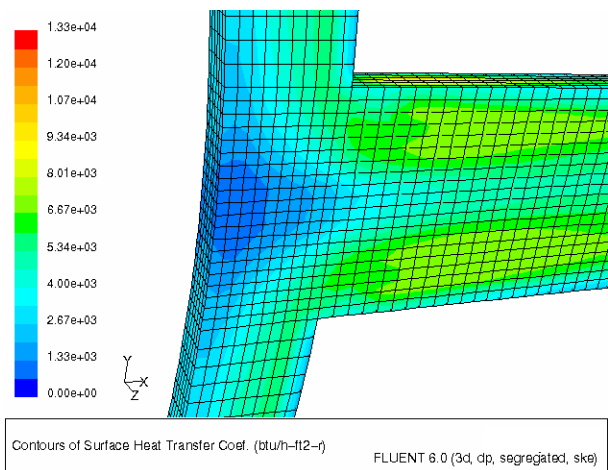


Figure 15. Flow rate = 0.7 lb/s contours of h (BTU/hr-ft²-R) near outlet.

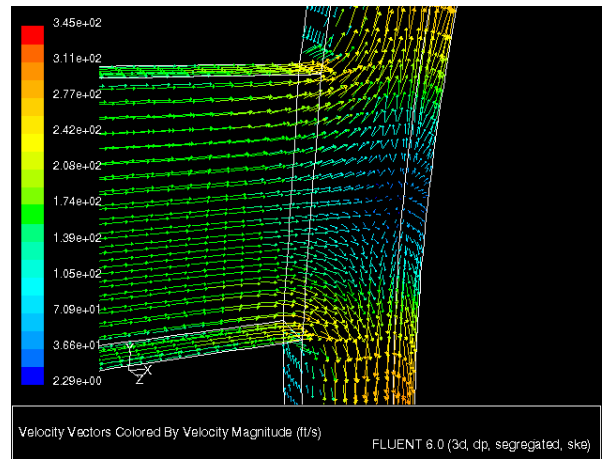


Figure 16. Flow rate = 1.0 lb/s velocity vectors near inlet.

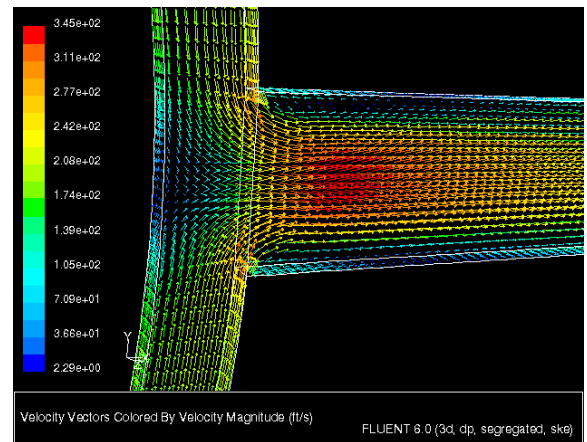


Figure 17. Flow rate = 1.0 lb/s Velocity vectors near outlet.

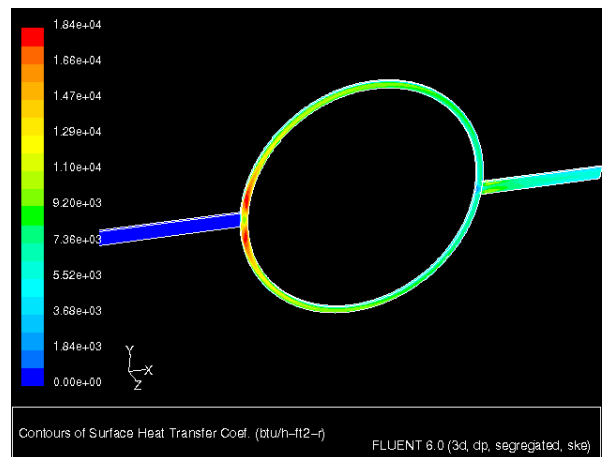


Figure 18. Flow rate = 1.0 lb/s contours of h (BTU/hr-ft²-R).

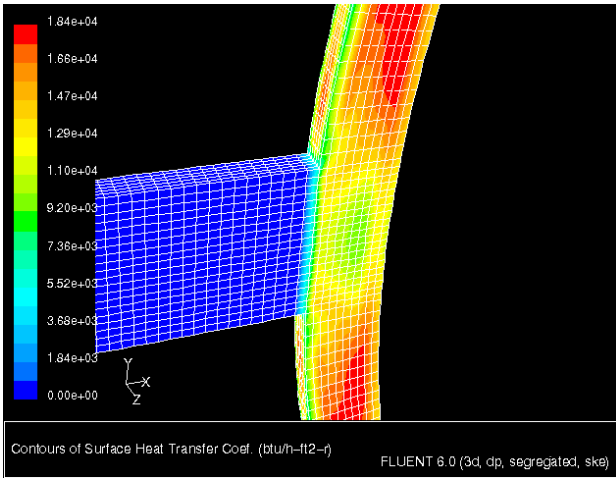


Figure 19. Flow rate = 1.0 lb/s contours of h (BTU/hr-ft²-R) near inlet.

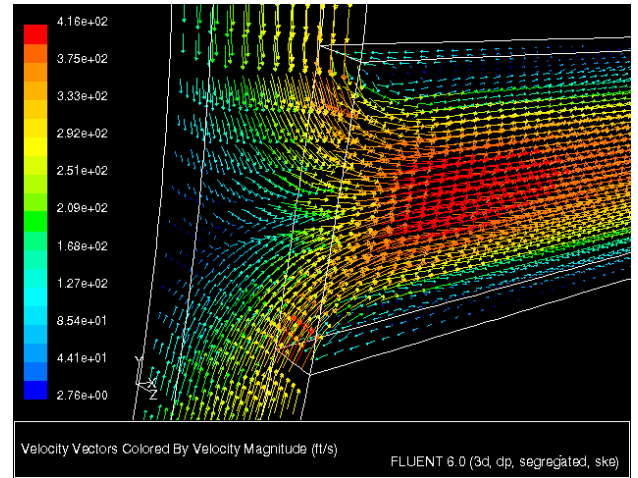


Figure 22. Flow rate = 1.2 lb/s velocity vectors near outlet.

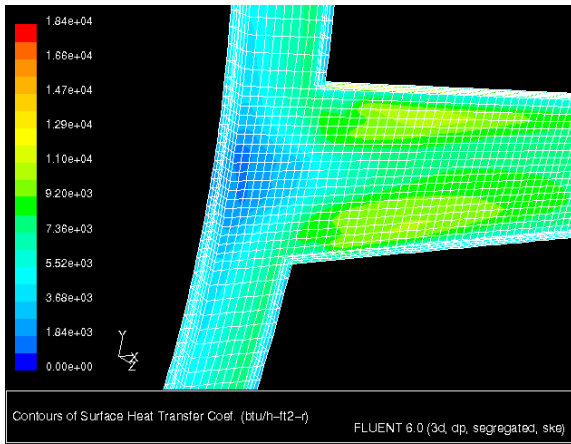


Figure 20. Flow rate = 1.0 lb/s contours of h (BTU/hr-ft²-R) near inlet.

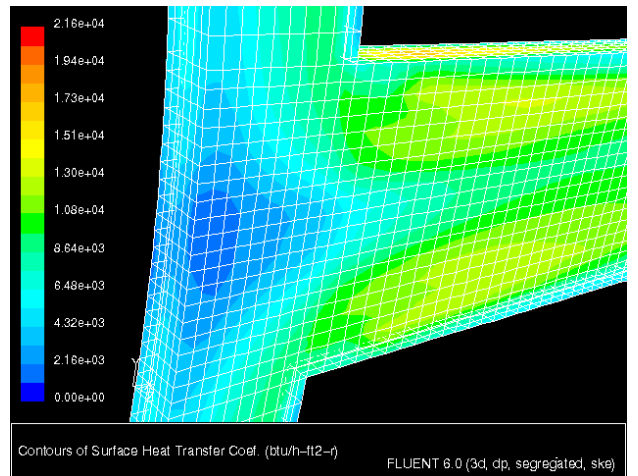


Figure 23. Flow rate = 1.2 lb/s contours of h (BTU/hr-ft²-R) near inlet.

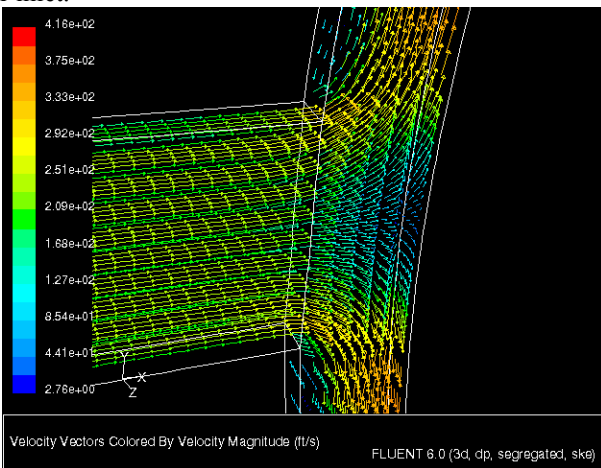


Figure 21. Flow rate = 1.2 lb/s velocity vectors near inlet.

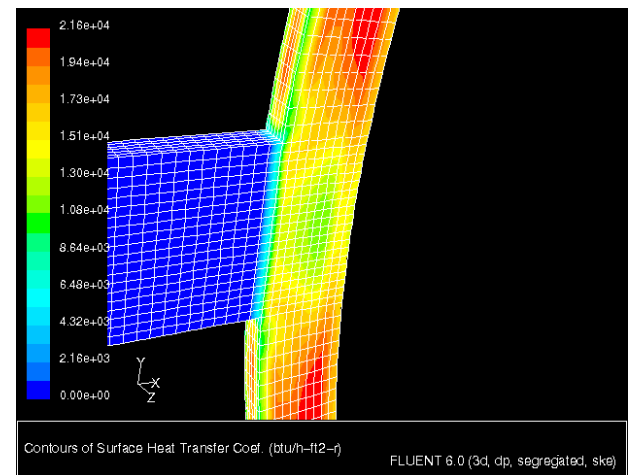


Figure 24. Flow rate = 1.2 lb/s contours of h (BTU/hr-ft²-R) near outlet.

The local film coefficient $h(x)$ was plotted as a function of its location along the streamwise length of the channel as shown in Figure 25.

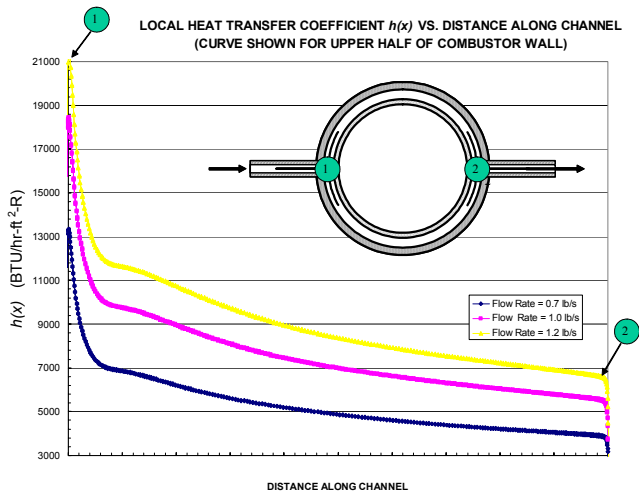


Figure 25. Local convective film coefficient versus location along the channel for various flow rates.

In Figure 25, each flow rate simulation is plotted, showing location 1, near the inlet, and location 2, near the outlet. In all cases, as expected, the heat transfer coefficient decreases by a factor of about 3, inlet to outlet. For example, the 1.2 lb/s flow rate case $h_{inlet} = 21,000$ BTU/hr-ft²-R at the inlet, and $h_{outlet} = 6,900$ BTU/hr-ft²-R at the outlet, the ratio being $\frac{h_{inlet}}{h_{outlet}} = 3.05$.

Similar ratios hold for the other two flow rates shown in Figure 25.

Finally, a summary of the area weighted average heat transfer coefficient, \bar{h} from each surface of the CFD model was constructed. This information is presented as Table 3 below.

Table 3. Summary of area weighted average heat transfer coefficients from combustor surfaces

FLUENT CFD Model Surface Description	Flowrate = 0.7 lb/s Area Weighted Average Surface Heat Transfer Coefficient (BTU/hr-ft ² -R)	Flowrate = 1.0 lb/s Area Weighted Average Surface Heat Transfer Coefficient (BTU/hr-ft ² -R)	Flowrate = 1.2 lb/s Area Weighted Average Surface Heat Transfer Coefficient (BTU/hr-ft ² -R)
combustorback	6448	8702	10541
combustorbottom	3986	5124	5815
combustorfront	6187	8885	10450
combustorinnerwall	5206	7507	8922
combustortop	3989	5159	5840
Net area weighted average	5868	8149	9681

The data of Table 3 support the findings of Figure 25, i.e. the larger the flow rate, the larger the film coefficient. This is seen by examining the last line of entries in Table 3, as the flow rate of LN2 increases from the minimum of 0.7 lb/s, to the maximum of 1.2 lb/s, the area weighted average film

coefficient increases from 5868 to 9681 BTU/hr-ft²-R. Thus, by increasing the coolant flow rate 71% a 65% increase in the heat transfer removal capability is realized.

CONCLUSION

The CFD analysis of inlet and outlet region of coolant channels in a prototype hydrocarbon engine has been presented herein. The analysis herein has been focused on one particular channel, that corresponding to the converging/diverging area of the combustor duct. The results found herein are expected to directly map to the other coolant channels, with the finding reported here being for the “worst-case” scenario. The methodology behind the CFD model has been presented. Parametric trades performed using the CFD model have shown that for a 71% increase in coolant supply rate, one obtains 65% more heat removal capacity. Also, the local heat transfer coefficient at the inlet of the coolant channel is approximately three times that of the outlet region.

REFERENCES

1. NIST 12 Thermodynamic and Transport Properties of Pure Fluids Database, <http://www.nist.gov/srd/nist12.htm>
2. “Introduction to Fluid Mechanics,” R.W. Fox and A. T. McDonald, 4th Ed. , McGraw-Hill, 1992, pg. 358.
3. Fluent 6.0 User’s Guide, 2001, Fluent, Inc., Lebanon, NH.